

# We are IntechOpen, the world's leading publisher of Open Access books Built by scientists, for scientists

6,900

Open access books available

185,000

International authors and editors

200M

Downloads

Our authors are among the

154

Countries delivered to

TOP 1%

most cited scientists

12.2%

Contributors from top 500 universities



WEB OF SCIENCE™

Selection of our books indexed in the Book Citation Index  
in Web of Science™ Core Collection (BKCI)

Interested in publishing with us?  
Contact [book.department@intechopen.com](mailto:book.department@intechopen.com)

Numbers displayed above are based on latest data collected.  
For more information visit [www.intechopen.com](http://www.intechopen.com)



# Bayesian Uncertainty Evaluation in Vision-Based Metrology

Markus Brandner  
Graz University of Technology  
Austria

## 1. Introduction

Metrology as the science of measurement is omnipresent in today's society. Many applications in a variety of fields ranging from economy to science have a strong demand for reliable methods to quantify and compare measurement results. Depending on the specific application, this comparison can cover measurements acquired within the same minute by the same operator using the same measurement instrument under the same environmental conditions, or measurements acquired within a month by different operators and measurement instruments on two different continents. In either case, metrology has to provide means to ensure the validity of the comparison of those measurement results. Two aspects of metrology are of importance to us in the context of this paper: The *traceability* of the measurement result and the evaluation of the quality of the measurement result by means of its associated *measurement uncertainty*.

**Traceability:** The measurement process is defined as a quantitative comparison of an unknown physical quantity - the *measurand* - with a known standard (cf. DIN1319 (1995)). Measurement results can thus only be compared on an international level provided compatible standards are available and used. Consequently, our society requires a world-wide system of physical standards which is accepted by and accessible to every nation. The first attempts to internationally standardise physical quantities date back to 1875, when the *Bureau International des Poids et Mesures* (BIPM) was founded on the basis of the Metre Convention (BIPM (2008)). At that time, international prototypes of the metre and the kilogram were physically built. The evolution of these references triggered the installation of seven base quantities. Since the 11<sup>th</sup> General Conference on Weights and Measurements in 1960, this system of base units is referred to as the *International System of Units* (SI) (BIPM (2006)). Today, standards are maintained and made available to the public of participating member states and associated economies by means of a hierarchical structure of international and national metrological institutes as outlined in Figure 1. The highest quality standards are available at BIPM and are used to derive secondary standards operated by national metrological institutions. These institutions, in turn, are responsible to pass standards on to subordinate laboratories and eventually to instrument manufacturers. This concept of *traceability* ensures that every measurement can be referred back to a physical standard by an unbroken chain of comparisons (International vocabulary of basic and general terms in metrology, VIM (1993)). An example of such a comparison chain is provided in Figure 2. An optical instrument is used to measure the position  $x$  of a

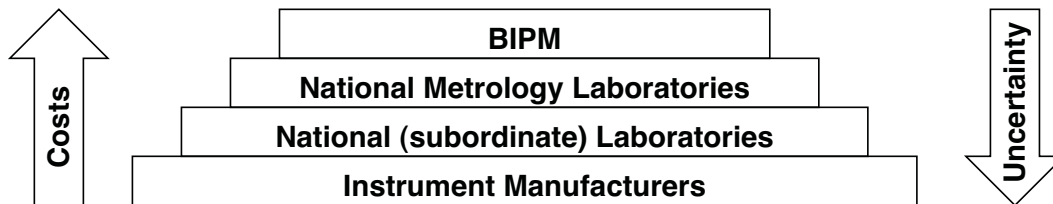


Fig. 1. Hierarchy of metrological institutions responsible to maintain the SI system. The costs and the quality of the standards kept at the different layers increase from bottom to top. Similarly, the uncertainty of the different standards increase from top to bottom. Any measurement taken by an instrument which is properly calibrated can now be traced back to the base standard kept at BIPM.

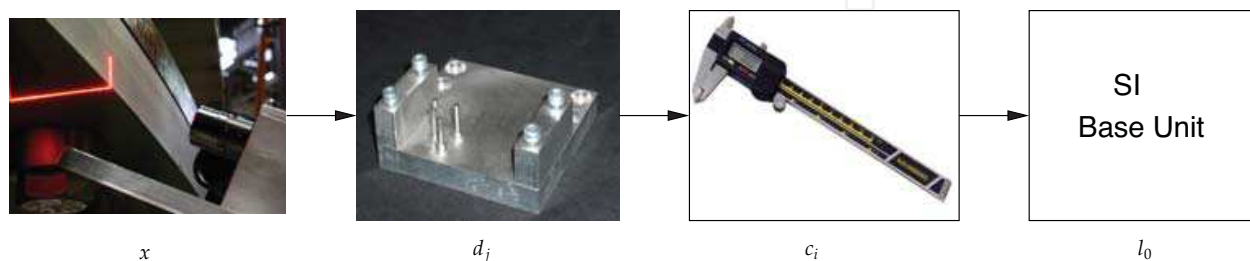


Fig. 2. The concept of traceability shown at the example of an optical measurement system. The length standard applied within the measurement system can be traced back to the meter standard.

mechanical part in 2D. A chain of comparisons links the measurement results of this instrument back to the length standard: The geometry of the instrument is calibrated using a calibration target. During this calibration procedure, the positions  $d_j$  of different geometric features such as bores and bolts serve as geometric references. These reference positions are determined during the manufacturing process of the target using a measurement device such as the shown calliper. By means of these measurements, the components of the vectors  $d_j$  are referred to the metric reference  $c_i$  of the calliper. Finally, the calliper is calibrated by the instrument manufacturer using standards that can likewise be referred to the length standard  $l_0$  – symbolised in this example by the image of the metal bar representing the metre standard. Consequently, the measurement results obtained using the optical instrument can be traced back to the metre standard. Only through this specific setting, the measurement results are of practical use within a manufacturing process based on the current SI. The lack of traceability in such an environment would inevitably lead to false tolerances and hence defective parts.

**Measurement Uncertainty (MU):** The BIPM defines metrology as ‘the science of measurement, embracing both experimental and theoretical determinations at any level of uncertainty in any field of science and technology’<sup>1</sup>, which highlights a second important aspect of metrology: the treatment of measurement uncertainty. The term *uncertainty of a measurement* refers to a parameter that is assigned to each measurement and represents the spreading of the measurement values ‘. . . that could reasonably be attributed to the measurand’ (VIM (1993)). While the measurement of a scalar quantity results in a single *best estimate*, uncertainties are commonly expressed by means of an interval around this best estimate. Figure 3 depicts this

<sup>1</sup> see also [www.bipm.org](http://www.bipm.org).

situation. The measurand  $Y$  is determined resulting in the best estimate  $y$ . Assuming that deviations around this best estimate are symmetrically distributed to either side of  $y$ , we obtain an interval parameterised by the *expanded uncertainty*  $U_y$ . The interval is assigned a coverage probability  $p$ , such that

$$\text{Prob}(\{y - U_y < Y \leq y + U_y\}) = p, \quad (1)$$

where common probabilities are chosen to lie in the range of  $p = 95\% \dots 99\%$ .

A frequent misconception outside the metrology community is the ambiguous use of the term *measurement error*. While the measurement uncertainty does not require the true value  $y_{\text{True}}$  of the measurand  $Y$  to be known, the *measurement error*, in contrast, is determined as

$$y_{\text{Error}} = y - y_{\text{True}}, \quad (2)$$

which can only be evaluated once  $y_{\text{True}}$  is available. As this is never the case for any physical measurement<sup>2</sup>, the measurement error is only seen as a theoretical concept with little practical implications.

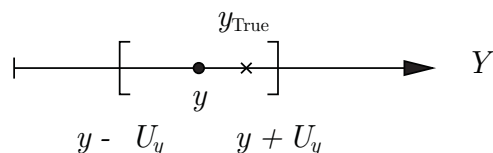


Fig. 3. The measurement uncertainty of a scalar measurand  $Y$  is expressed by an interval around the best estimate  $y$  which is parameterised by a coverage probability.

### 1.1 Vision-based measurement systems

Optical metrology utilises the interaction of light with an object in order to measure unknown quantities. Measurement principles based on the propagation of light are inherently non-contacting and mostly non-invasive. Thus, optical metrology is frequently used in applications where the measurand can either not be physically connected to a sensor (e.g. the measurement of mechanical stress and strain on a rotating blade of an aircraft turbine) or feedback of the measurement system to the measurand has to be kept to a minimum (e.g. measurements in the nano-scale). Further benefits of optical metrology include the potential to operate in large measurement volumes as well as the ability to set the focus of the measurement precisely at the point of interest through the line-of-sight principle that applies to light rays. While the large field of optical metrology covers the use of different light sources, sensors, and measurement principles, a sub-class of optical measurement systems uses 2D digital sensors to capture images and to perform signal processing on these images in order to deduce geometric properties of scenes or derived measurands. This sub-class is referred to as the class of *vision-based measurement systems*. Historically, these systems are also known as digital photogrammetric systems. In the context of this paper we refer to vision-based measurement systems with the following properties:

- Digital images are acquired using 2D image sensors (cameras).
- Greylevel features are used as primary source of information.

<sup>2</sup> The situation is different for simulation experiments, where  $y_{\text{True}}$  might be given.

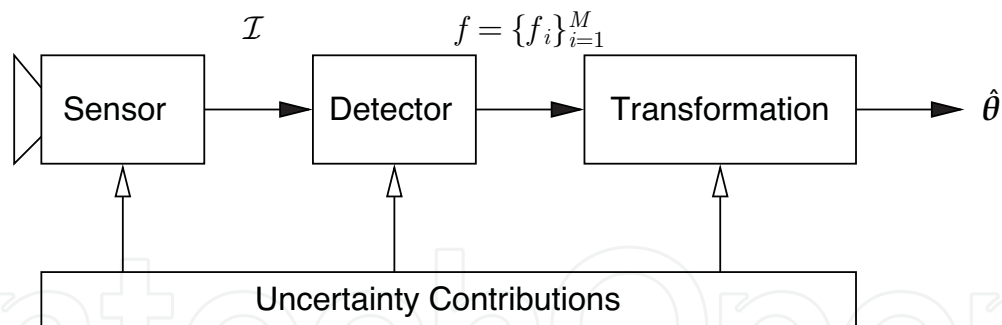


Fig. 4. Components of a typical vision-based measurement system. The best estimate of the unknown quantity  $\hat{\theta}$  is obtained given an 2D intensity profile  $\mathcal{I}$  acquired by the sensor.

- These features are used to derive measurands and their uncertainties.
- The measurement results are traceable to a standard and uncertainty estimates are provided.

The typical processing steps found in such systems are sketched in Figure 4: The camera maps the scene onto its image plane and acquires a 2D intensity profile  $\mathcal{I}$ . A feature detector is then used to identify features  $f$  (e.g. circular blobs) and to estimate their respective parameters (e.g. blob area and centre of gravity). These parameters are then being further processed by means of a transformation in order to obtain the best estimate of the unknown parameter  $\theta$ .

Two examples of vision-based measurement systems are shown in Figure 5. A close-up of the inside of a two-camera system used to measure 2D displacements is shown in Figure 5a. Traceability and the proper characterisation of measurement uncertainties in this application are of importance as the measurement results are used in a research project aiming at the investigation of the long-term behaviour of different materials. A proper decision taken on the basis of these measurements has a significant economic impact on the customer.

The Augmented Reality (AR) system shown in Figure 5b augments a user's view of the real world by adding computer generated content that is spatially registered with the real content. In this application, a monocular vision-sensor provides position and orientation (i.e. pose) data that are fused with data obtained by an inertial measurement unit mounted on the same rigid platform. The temporal stream of poses is further used by the AR software to render artificial content within the user's field of view. The successful information fusion in this particular setup requires all sensor data to be referred to the same length and time standards. As far as vision-based pose estimation is concerned, this prerequisite is achieved by a vision-based measurement system.

## 1.2 Related work

Efforts have been undertaken in metrology in order to develop a general framework that can be used to identify the quantity of the measurand and to provide means to judge on the quality of this result. These developments led to the introduction of the *Guide to the Expression of Uncertainty in Measurement* (GUM, most recent document JCGM (2008a)). The foremost aim of the GUM developments was to provide a recommendation for the treatment of measurement uncertainty that is *universal, internally consistent, and transferable* (JCGM (2008a)).

The standard GUM extensively uses the concept of *degrees of freedom* to fuse information from different sources. This concept is a constant point of criticism in the literature (cf.

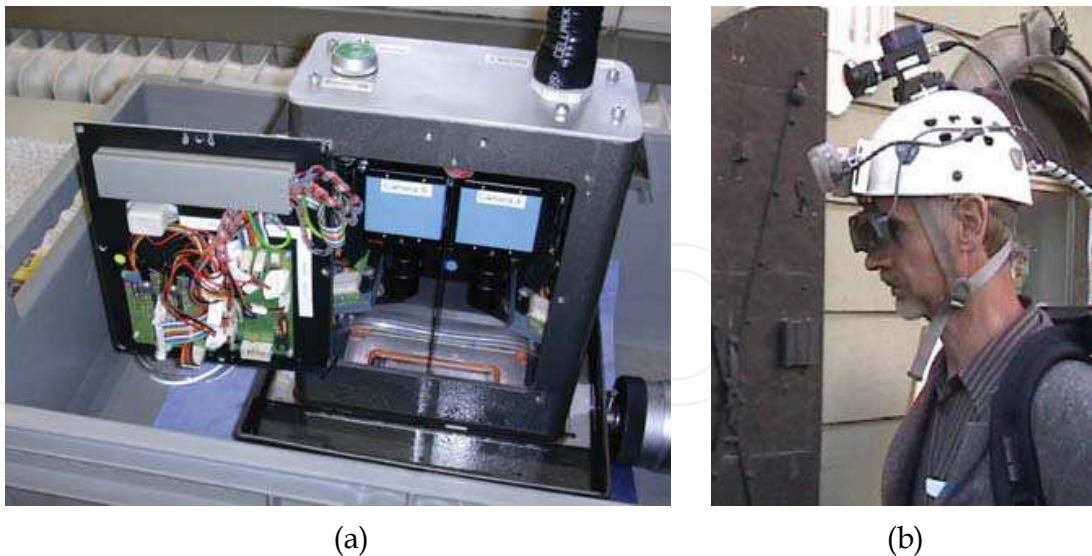


Fig. 5. Vision-based measurement systems. (a) Measurement application used to measure displacement and creep of material samples. (b) Vision-based pose estimation applied to Augmented Reality.

Lira (2001)). In particular, the fusion of quantities derived using statistical methods (e.g. averaging over a number of measurements) with quantities denoting an expert opinion (e.g. prior knowledge about interval boundaries) are not satisfactorily covered by the GUM proposal. Weise & Wöger (1999) and later Kacker & Jones (2003) resort to the consistent use of Bayesian statistics in the context of uncertainty computations. Both approaches remove an inconsistency in the GUM interpretation of coverage probabilities. Kacker & Jones (2003) provide a modified set of rules based on the GUM recommendations that are built upon the Taylor approximation of the measurement equation. Their proposed modifications cover the propagation of first and second order moments neglecting modifications of the underlying distributions. Weise & Wöger (1999) instead propagate distributions providing a framework that is more generally applicable. The recent *GUM Supplement 1* document (GUMS1, JCGM (2008b)) makes explicit the Bayesian foundations of the GUM. Thus removing inconsistencies in the information fusion of the guide.

Different approaches to the treatment of uncertainty in the domain of computer vision have been reported in the literature (e.g. Havelock (1989); Kanungo et al. (1995); Triggs (2001); Ochoa & Belongie (2006)). Using the central limit theorem (CLT, Papoulis & Pillai (2002)) as a key argument, the use of the Gaussian assumption is suggested – and often validated – by many researchers. Heuel (2003) and Criminisi (2001) show that Gaussian densities can be applied to represent homogeneous geometric entities. In an earlier work (Brandner (2006)) we apply first order propagation of Gaussian quantities to a vision-based tracking application. Based on the exclusive use of Gaussian densities to describe both physical quantities and prior information, the Bayesian extensions of the GUM document are easily implemented in analytic form.

From a practical point of view, the proper evaluation of measurement uncertainties relies on the quality of the underlying process model. In many situations these models are complex and not straight-forward to derive. Sommer & Siebert (2006) propose a systematic solution to the model building problem in metrology. The authors use three building blocks to identify and visualise influencing factors and uncertainty contributions. Based on the cause-

and-effect approach, *Parameter Sources*, *Transmission Units*, and *Indicating Units* are employed to obtain the measurement equation. This equation is then reversed to obtain the GUM-compliant model equation. Finally, the measurement uncertainty of the unknown quantity can be derived.

### 1.3 Contribution

In this work we fuse the existing Gaussian characterisation of geometric entities within the field of uncertain perspective geometry with the uncertainty concepts of the GUM document. In order to highlight the quality of the obtained geometric quantities this concept is referred to as *metrological geometry*.

We present a modelling technique based on the cause-effect diagram which makes explicit the statistical dependencies between different geometric entities. Further, we show that for many problems in vision-based metrology an analytic frame-work for the propagation of Gaussian uncertainties can be applied. All processing steps can be carried out analytically, thus avoiding any simulation-based computations with the potential lack of real-time performance. The frame-work is consistent with the Bayesian extensions to the standard GUM. Using a number of simple building blocks we propose simple modelling steps to analytically derive the measurement uncertainty in vision-based applications explicitly covering inter-parameter dependencies.

The remainder of this chapter is structured as follows: based on a brief review of the GUM recommendations in the following Section 2 we introduce a common nomenclature and derive the requirements for a vision-based metrological application in Section 3. The subsequent Section 4 presents our approach to the modelling process and introduces the basic building blocks of a vision-based measurement system which are then applied to a simple example in Section 5. The paper concludes with a summary in Section 6.

## 2. The guide to the expression of uncertainty in measurement

Given a measurement process, the current GUM represents a general frame-work that can be used to evaluate the uncertainty of a physical quantity that results from that measurement. However, the GUM does not provide any means to determine appropriate models. In the following paragraphs we review the basic concepts of the GUM in order to provide the background required to develop the concept of the metrological geometry in Section 4.

### 2.1 Uncertain quantities

Assuming a measurand denoted by  $Y$  depends on a number of input quantities  $X_i$ , the GUM frame-work allows us to determine the uncertainty of a measurement result  $y$  taking into account the uncertainties of the contributing input quantities. Quantities in this context are treated as variables and their uncertainty is represented by a state-of-knowledge distribution. The best estimate of a quantity  $Y$  and its uncertainty are represented by the mean value and the standard deviation of the underlying PDF  $f_Y(\cdot)$ , respectively. Thus, the best estimate of the measurand  $Y$  is given by

$$E\{Y\} = \mu_Y = \int_{-\infty}^{+\infty} \eta f_Y(\eta) d\eta \quad (3)$$

and the associated standard deviation is given by

$$\sigma_Y = \sqrt{E\{[Y - \mu_Y]^2\}}. \quad (4)$$

Depending on the method used to determine the uncertainty of input quantities the GUM distinguishes between two families of uncertainty evaluations: *Type A* uncertainties are determined by statistical methods while uncertainties obtained *by other means* are classified as *Type B*.

The determination of a quantity  $Y$  by means of  $N$  repeated independent observations<sup>3</sup>  $y_i$  represents an example of a *Type A* uncertainty evaluation. The estimated arithmetic mean value of the observations is given by

$$\bar{y} = \frac{1}{N} \sum_{i=1}^N y_i \quad (5)$$

and the associated standard deviation of the arithmetic mean  $\bar{y}$  is given by  $s_{\bar{y}} = s / \sqrt{N}$ , where  $s$  denotes the empirical standard deviation of the observations and is given by

$$s = \sqrt{\frac{1}{N-1} \sum_{i=1}^N (y_i - \bar{y})^2}. \quad (6)$$

The GUM recommends to use the arithmetic mean  $\bar{y}$  as best estimate for the quantity  $Y$  and to use the standard deviation  $s_{\bar{y}}$  as *standard uncertainty*<sup>4</sup>  $u_{\bar{y}}$ .

*Type B* uncertainties are used to treat input quantities whose uncertainty is determined by methods other than statistics. An example is the uncertainty associated with the calibration of an instrument. In this case best estimate, standard uncertainty, and degrees of freedom are given by the calibration laboratory. Other examples are the uncertainty of the transformation parameters and the detector used in the above example of a vision-based measurement system. In both cases the characterisation of the uncertainty is based on the experience of the experimenter and, thus, on *non-statistical* evaluations.

## 2.2 The measurement process

The evaluation of the uncertainty associated to the measurand is based on a mathematical model

$$Y = f(X_1, X_2, \dots, X_N) \quad (7)$$

of the measurement process, where  $Y$  denotes the measurand and the  $X_i$  represent input quantities. This relation is referred to as the *model equation*. The best estimate of the measurand is given by replacing all input quantities in Equation 7 by their respective best estimates such that

<sup>3</sup> We will use the terms observation and measurement interchangeably.

<sup>4</sup> Following a suggestion by Sommer & Siebert (2006) we use  $u_{\bar{y}}$  as symbol for the standard uncertainty associated to the measurement result  $\bar{y}$  rather than the GUM nomenclature  $u(\bar{y})$  which suggests that the standard uncertainty is a function of the best estimate.



$$y = f(x_1, x_2, \dots, x_N). \quad (8)$$

Based on the estimates of the input values and their associated standard uncertainties, the *standard uncertainty*  $u_y$  is derived. Summarising the input quantities and their best estimates into a vector  $X = (X_1, X_2, \dots, X_N)^T$  and a vector  $x = (x_1, x_2, \dots, x_N)^T$ , respectively, the measurement equation is developed into a Taylor series to obtain (cf. Weise & Wöger (1999))

$$Y = f(\mathbf{X}) \approx f(\mathbf{x}) + \sum_{i=1}^N \frac{\partial f(\mathbf{x})}{\partial X_i} (X_i - x_i) + \quad (9)$$

$$+ \sum_{i=1}^N \sum_{j=1}^N \frac{\partial^2 f(\mathbf{x})}{\partial X_i \partial X_j} (X_i - x_i)(X_j - x_j) + \dots \quad (10)$$

Assuming small deviations  $(X_i - x_i)$ , the higher order terms of the Taylor expansion are neglected leading to the simplified approximation

$$Y \approx f(\mathbf{x}) + \sum_{i=1}^N \frac{\partial f(\mathbf{x})}{\partial X_i} (X_i - x_i). \quad (11)$$

The partial derivatives of the measurement equation are referred to as *sensitivity coefficients*  $c_i = \frac{\partial f(\mathbf{x})}{\partial X_i}$ . Using Equation 11, the variance of the measurement result  $y$  is obtained by

$$u_y^2 = \left( E \left\{ \sum_{i=1}^N c_i (X_i - x_i) \right\} \right)^2 = \sum_{i=1}^N c_i^2 u_{x_i}^2 + 2 \sum_{i=1}^{N-1} \sum_{j=i+1}^N c_i c_j \rho_{ij} u_{x_i} u_{x_j}, \quad (12)$$

with  $u_{x_i}$  denoting the standard uncertainties of the input values. The correlation coefficients  $\rho_{ij} = \text{Cov}(x_i, x_j) / u_{x_i} u_{x_j}$  account for inner dependencies of the contributing input values. As  $u_y$  results from combining the input parameter uncertainties it is called the *combined standard uncertainty* of the measurement result  $y$ .

The GUM further suggests to report an interval within which a large fraction  $p$  of the distribution of values attributed to the measurand  $Y$  fall. Given a symmetric distribution of  $Y$ , this interval is obtained through the symmetrical extension of the best estimate  $y$  by the *expanded uncertainty*  $U_y$  to either side as shown for a scalar quantity in Figure 3. Assuming knowledge about the distribution of  $Y$ , the expanded uncertainty is obtained by  $U_y = k \cdot u_y$  where  $k$  is a coverage factor. The fraction  $p$  is denoted the *level of confidence* associated to the *coverage interval* ( $y \pm U_y$ ).

The uncertainty estimates are based on realisations of random variables and, therefore, are subjected to uncertainty, too. Only for the evaluation of the expanded uncertainty, the standard GUM uses the concept of degrees of freedom of the input quantities and suggests to estimate an *effective number of degrees of freedom* of the resultant distribution based on the Welch-Satterthwaite (WS) equation (JCGM (2008a)).

### 2.3 Bayesian evaluation of measurement uncertainties

The standard GUM document has often been a target of criticism due to the lack of a clear distinction between the use of classical statistics and Bayesian statistics in the evaluation of measurement uncertainties. As opposed to the classical statistics approach which treats measurands as constants and the observations (e.g. made during Type A evaluations) as

realisations of random variables with known distributions, Bayesian statistics is built upon the philosophy that the measurand is itself a random variable and the observations are seen as constants (Kacker & Jones (2003); Gelman et al. (2003)). The important difference between the two approaches is that the state-of-knowledge distribution in the Bayesian theory does not represent an approximation but is assumed to be exact. Consequently, there is no uncertainty involved in evaluating the coverage intervals. Classical statistics, on the other hand, requires the handling of degrees of freedom and their controversial combination by means of the WS equation. In the Bayesian theory the state-of-knowledge of every quantity is given by distributions which must not be confused with frequency distributions in the sense of classical statistics (Weise & Wöger (1999), p.225). Prior knowledge about quantities and their associated lack of knowledge is represented by prior distributions (or simply: priors). In the case of complete lack of knowledge, these distributions are replaced by non-informative priors (Iversen (1984); Gelman et al. (2003); Jaynes (1968)).

Recently, the Supplement 1 document clearly shows that the GUM concept of measurement uncertainty evaluation is based on the Bayesian idea. We will subsequently refer to the fully Bayesian interpretation of measurement uncertainties as GUM/Bayes.

#### 2.4 Multidimensional measurands

The concept of GUM/Bayes as presented above straight forwardly extends to multiple dimensions (cf. Lira (2001)). During this extension the best estimate of a vector-valued quantity is given by the mean vector comprising the expected values of the individual components. Thus, for a vector-valued quantity

$$\mathbf{Q} = (Q_1, Q_2, \dots, Q_n)^T \quad (13)$$

the best estimate is given by the mean vector

$$\boldsymbol{\mu}_q = E\{\mathbf{Q}\} = (E\{Q_1\}, E\{Q_2\}, \dots, E\{Q_n\})^T = (\mu_{q_1}, \mu_{q_2}, \dots, \mu_{q_n})^T. \quad (14)$$

The standard uncertainty of the scalar quantity is extended towards the *uncertainty matrix*

$$U_q = \Sigma_{QQ} + (E\{\mathbf{Q}\} - \mathbf{q})(E\{\mathbf{Q}\} - \mathbf{q})^T, \quad (15)$$

where  $\Sigma_{QQ}$  represents the covariance matrix of the measurand. Equation 15 covers the general case of arbitrary estimates  $\mathbf{q}$ . Using unbiased estimators, the uncertainty matrix simplifies to

$$U_q = \Sigma_{QQ}. \quad (16)$$

These extensions suffice to determine the combined standard uncertainty of the measurement result. Analogous to the scalar case the expanded uncertainty represents a multidimensional interval. Based on an  $n$ -dimensional measurand  $\mathbf{Q} \in S^{(n)}$ , where  $S^{(n)}$  denotes the  $n$ -dimensional space, Iuculano et al. (2003) extend the concept of an coverage interval as defined in the GUM to a limited domain  $C^{(n)} \in S^{(n)}$ . Assuming the PDF of the measurand is denoted by  $f_Q(\cdot)$  the coverage probability associated with  $C^{(n)}$  is given by

$$p = P\{\mathbf{Q} \in C^{(n)}\} = \int_{C^{(n)}} f_Q(\mathbf{q}) d\mathbf{q}. \quad (17)$$

It is not *a priori* defined what the shape of such a region in  $S^{(n)}$  looks like. The GUM suggests to apply two criteria for the choice of the interval boundaries: the minimum width interval or the interval given by equal density values. While the recommendation for Monte Carlo (MC) simulation in the Supplement 1 document JCGM (2008b) suggests to revert to the minimum width interval for general densities, this can not be straight forwardly applied to  $S^{(n)}$ . Restricting our attention to multidimensional Gaussian distributions we find that ellipses (or hyper-ellipsoids in higher dimensions) meet the requirements of coverage regions. These regions are delimited by contours of constant density and are consistent with the GUM suggestions. This choice is supported by Iuculano et al. (2003) who show for square and circular regions  $C^{(n)}$  that the analytically derived coverage probabilities for Gaussian and uniform distributions are in agreement with ground truth data obtained from Monte Carlo simulations.

### 3. Requirement analysis for a measurement uncertainty frame-work

In order to identify the requirements for an uncertainty propagation frame-work we use the following measurement example: A vision-based measurement system is used to measure the 2D displacement of a mechanical lever. In order to robustly capture the displacement, a circular blob marker is attached to the lever. This marker now translates within a known plane which is fixed with respect to a perspective sensor. The goal of the measurement process is to estimate the position of the marker and, consequently, the displacement of the lever in world coordinates based on measurements taken in the sensor image. We restrict this example to a measurement based on a single image acquisition. The uncertainty associated with this estimate must be identified. Figure 6 shows a sketch of the geometry of the measurement system.

The blob marker is represented by its centre vector  $\mathbf{p} = (x, y)^T$ . The allowed set of positions is restricted to lie within the plane  $\Pi_{\text{World}}$  by construction of the measurement system. The sensor now maps the blob onto the image plane  $\Pi_{\text{Image}}$ . In order to measure the position of the lever the following processing steps are performed: a single image is acquired, the blob centre  $\mathbf{a} = (u, v)^T$  is estimated, and the corresponding centre  $\mathbf{p}$  is determined. The points  $\mathbf{p}$  and  $\mathbf{a}$  are related to each other by means of a parameterised transformation function

$$\mathbf{p} = g(\mathbf{a}; \theta), \quad (18)$$

where  $\theta$  denotes the parameter vector characterising the measurement setup. For every practical realisation of the above example the measurement result is subjected to uncertainties. Important sources of uncertainty can be found in every processing step, e.g.

- *Sensor*: After the mapping of the marker onto the sensor plane using principles of geometric optics the sensor performs both a spatial and an intensity discretisation. The effects of this discretisation steps can be modelled by means of additive noise sources.
- *Detector*: Although blob detection may seem to be straight forward at a first glance, it already exhibits a fundamental problem in optical metrology: it is, in general, not possible to accurately model the image acquisition system which is a prerequisite for the estimation of parameters such as the blob centre. We assume in this example that the uncertainty introduced by the blob detector is characterised by the experimenters experience.

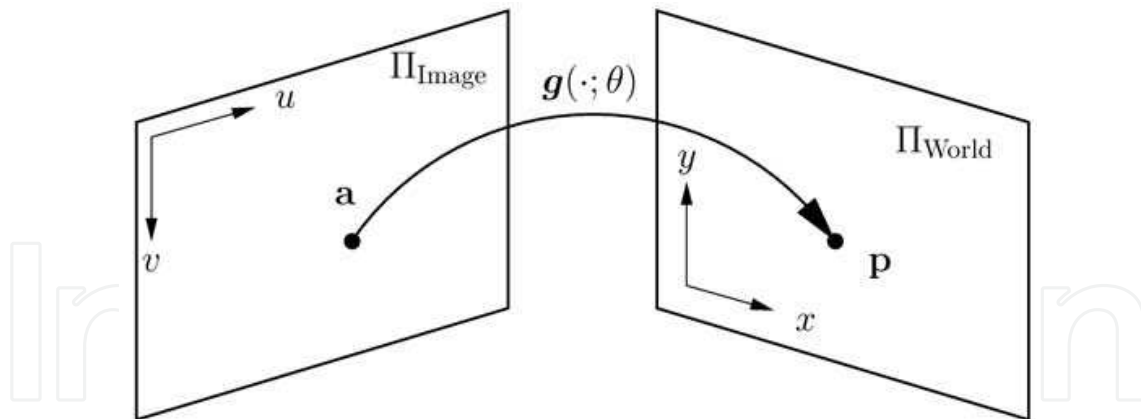


Fig. 6. Example application: The position of a point  $\mathbf{p}$  in world coordinates is based on a detected point centre  $\mathbf{a}$  in image coordinates. Both coordinate systems are related to each other by means of a transformation function  $g(\cdot; \theta)$ .

- *Transformation:* The measurement of  $\mathbf{p}$  requires that the parameters of the transformation  $g(\cdot; \theta)$  are known in advance. Given that these parameters necessarily are obtained by a calibration procedure they are subjected to uncertainties, too. Commonly, the parameter vector  $\theta$  is assumed to be a realisation of a random process and the corresponding moment estimates are obtained during the calibration process.

Using this example we can already identify the requirements on a frame-work for the treatment of uncertainties which will later be applied to vision-based metrology applications. The following properties are required:

1. *Treatment of multivariate measurands:* Many of the measurands in the vision-based metrological application are multivariate variables such as point positions or parameters of a line.
2. In particular, many of the geometric entities are represented in a projective space. Consequently, the uncertainty frame-work needs to properly cover multivariate variables.
3. *General applicability to geometric entities:* In order to be of general use in the given context the uncertainty frame-work is required to be applicable to geometric entities of any type.
4. *Common handling of different types of input uncertainties:* As shown in the example there are two distinct types of uncertainties to be taken into account when computing the uncertainty of the measurement result: input parameter uncertainties such as noise effects that are described by means of statistics and uncertainties that are given based on experience. An example of the later class of uncertainties are general judgements on the quality of the calibration of a measurement setup.
5. *Propagation through different processing blocks:* Even this simple example consists of several processing blocks covering the sensor transfer function, feature detection, and the subsequent application of the transformation.
6. *Processing speed:* While in many metrological applications the determination of uncertainties can be solved off-line using simulation-based approaches, some applications require the real-time determination of parameter uncertainties. Examples include measurement systems with a varying number of input parameters. As opposed to simulation-based approaches, an analytical method can usually meet the processing speed requirements as it has a fixed processing time and is of lower complexity.

7. *Single measurements:* Repeated measurements are generally used to reduce the contribution of random effects. This requires that the measurements can be repeated under similar conditions. The relatively large sampling intervals and the amount of data being processed within a single image puts a limit on the minimum time interval between two consecutive acquisitions in vision-based applications. Thus, single measurement situations are frequently encountered in vision-based metrology which calls for a specific treatment of measurement uncertainty.
8. *Dealing with correlations:* Features extracted from a single image inherently show a certain degree of correlation due to the common conditions under which the image has been acquired. These correlations can have a significant impact on the uncertainty of the measurement result.

#### 4. Metrological geometry

Homogeneous coordinates are frequently used in computer vision to represent geometric entities (Hartley & Zisserman (2004)). In contrast to the Euclidean representation, entities in projective spaces lead themselves to simple formulations and constructions. Given prior work by Criminisi (2001), Heuel (2003), and Förstner (2004) we observe that a multivariate Gaussian model is applicable to the problem of representing homogeneous entities in projective spaces. Using the bilinear transformation to construct new entities, this specific representation of parameter uncertainty provides a consistent tool. However, the validity of the approach only covers situations where the mean values of the parameters are large compared to their standard deviations. Heuel (2003) discusses conditions which suffice to obtain bounded parameter biases. By itself, the concept of uncertain projective geometry does not represent a frame-work for a proper expression of uncertainties. The missing elements cover the proper interpretation of a PDF as well as the metrologically sound derivation of standard, combined, and expanded uncertainties based on parameter densities. These elements are provided by GUM/Bayes as shown in Section 2 for the general case of multivariate quantities. In particular, GUM/Bayes covers the incorporation of prior knowledge and the appropriate treatment of correlated quantities.

Although most of the integrations suggested by GUM/Bayes can only be solved through time-consuming numerical algorithms such as Monte Carlo integrations, the restricted subset of quantities modelled by multivariate Gaussian densities leads itself to solutions which can be obtained analytically. If we further restrict any prior information to be represented by Gaussian quantities, we obtain a frame-work for the treatment of uncertain quantities based on the propagation of first- and second-order moments.

Consequently, we propose a fusion of the uncertain projective geometry with the GUM/Bayes approach in order to derive the concept of *metrological geometry* as outlined in Figure 7. Combining the ideas of uncertain projective geometry with the GUM/Bayes approach to the treatment of measurement uncertainty allows us to simplify and unify the modelling process for problems in geometric metrology. In summary our approach covers the following situations:

- Homogeneous entities represented by Gaussian random vectors. For example, a homogeneous point in 2D is given by

$$\underline{\mathbf{x}} \sim \mathcal{N}(\underline{\mathbf{x}}, \underline{\Sigma}_{\underline{\mathbf{x}}}). \quad (19)$$

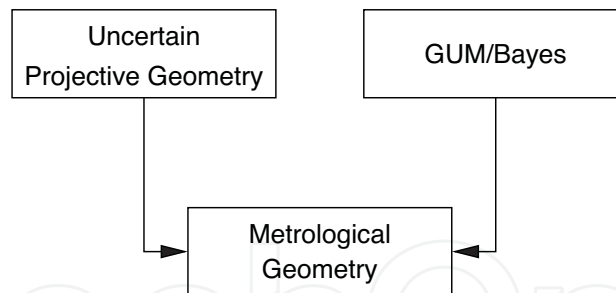


Fig. 7. Uncertain projective geometry and GUM/Bayes are combined to obtain a consistent frame-work for the treatment of uncertainties in vision-based metrological applications.

- Mapping of homogeneous entities including the propagation of parameter uncertainties. Mapping functions include: geometric transformations such as translations, rotations, and perspective mappings. Further, geometric construction (e.g. point results from intersecting two lines) and Euclidean and spherical normalisation are covered.
- Measurement updates of geometric entities with prior knowledge based on Gaussian random vectors.
- Correlations between geometric entities.

As opposed to the general recommendations provided by the original GUM document, the determination of the measurement uncertainty can be greatly simplified when considering only Gaussian uncertainties. Only a small number of building blocks is required to obtain a valid metrological model following a simple modelling procedure.

In the subsequent paragraphs we propose a unified nomenclature and present guidelines which cover the basic steps required to identify the model equation for vision-based metrological problems. In particular, we introduce components of a graphical model which greatly simplifies the setup of the model equation.

#### 4.1 Nomenclature in metrological geometry

The nomenclature used in uncertain projective geometry differs from the nomenclature used in the GUM document. In particular, the GUM denotes physical quantities by upper case letters and their realisations (e.g. measurement results) by the corresponding lower case letters. While uncertain projective geometry uses covariance matrices for multivariate entities, the GUM document distinguishes between standard, combined, and expanded uncertainties in the univariate case and provides an uncertainty matrix in the multivariate case.

In the subsequent modelling process, we will use a unified nomenclature which assigns underlined symbols to quantities in a metrological sense. Their corresponding non-underlined version is used to denote realisations of the quantity. If it is clear from the context, we will also use the non-underlined symbols to denote the best estimates of the corresponding quantities. Thus,  $\underline{c}$  is a scalar quantity and  $c$  is the corresponding realisation or best estimate. Following GUM we use  $u_c$  to denote the standard uncertainty of the best estimate and  $U_c$  as expanded uncertainty associated to a given coverage factor  $k$ . Similarly, a vector-valued quantity is referred to as  $\underline{\mathbf{x}}$ . The best estimate of  $\underline{\mathbf{x}}$  is given by  $\mathbf{x}$ . The uncertainty matrix  $U_{\mathbf{x}}$  of  $\mathbf{x}$  corresponds to the covariance matrix  $\Sigma_{\underline{\mathbf{x}}}$  of the quantity. It is now straight forward to make explicit the correlation between two different quantities  $\underline{m}$  and  $\underline{n}$  by means of their cross-covariance matrix  $\Sigma_{\underline{mn}}$ . The multivariate equivalent to the expanded

uncertainty is obtained by finding constant density curves of the PDF which corresponds to a given coverage probability  $p$ . For 2D Gaussian quantities these curves are ellipses of general orientation as outlined for different coverage probabilities in Figure 8.

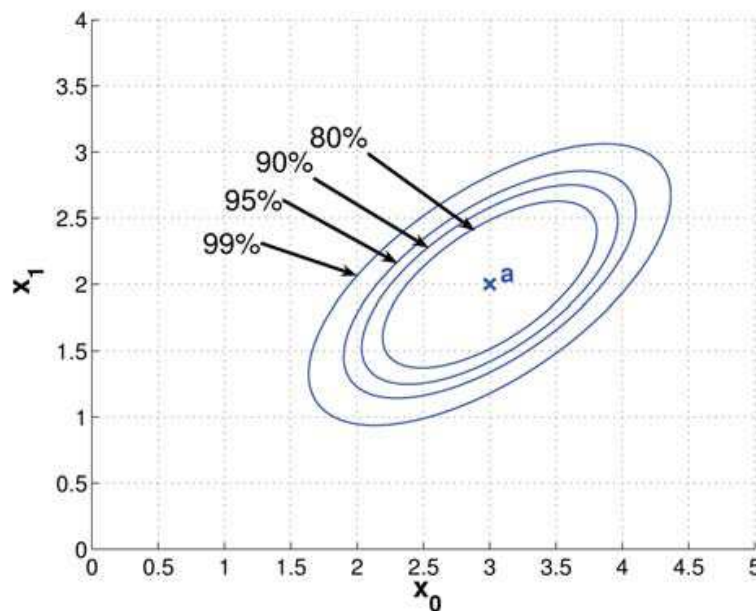


Fig. 8. Visualisation of the expanded uncertainty of a 2D Gaussian quantity  $\underline{a}$ . Curves of constant probability density are ellipses in general configuration centred around the best estimate  $\underline{a}$ . Different regions for varying coverage probabilities are shown.

#### 4.2 The modelling process

The model equation as given by Equation 7 expresses the functional relationship between the measurand  $\underline{Y}$  and the input quantities  $\underline{X}_1, \dots, \underline{X}_N$ . However, the structure of the model equation usually does not directly reflect the processing steps involved in the measurement process. If we assume that the measurand  $\underline{Y}$  is determined by reading the result of the quantity  $\underline{X}_3$ , Equation 7 can be reformulated such that  $\underline{X}_3$  is given by

$$\underline{X}_3 = f_M(\underline{Y}, \underline{X}_1, \underline{X}_2, \underline{X}_4, \dots, \underline{X}_N), \quad (20)$$

which is referred to as the *measurement equation*. Sommer & Siebert (2006) suggest to base the model building process on this measurement equation as it physically relates the *cause*, i.e. the measurand  $\underline{Y}$ , to an *effect*, i.e. the reading  $\underline{X}_3$ . We propose to perform the following steps in order to evaluate the measurement uncertainty of a vision-based metrology system using this model equation:

- **Description of the Measurement Task:**

A complete description of the measurement task is the most important step of the modeling process. This description includes the input quantities and – most importantly – the measurand.

- **Cause-Effect Relations:**

All quantities included in the above description must be brought into a form following the idea of the cause-effect approach. It is helpful to visualise these relations using a simple graph as shown in Figure 9.

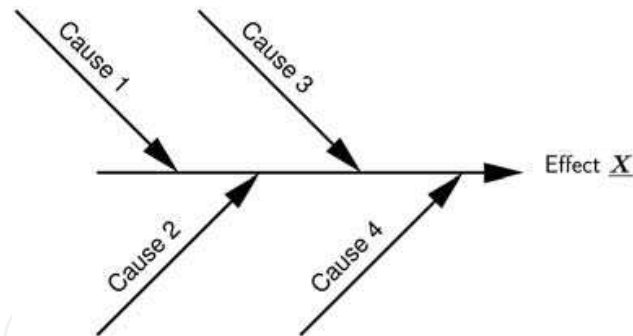


Fig. 9. Graphical representation of the cause-effect relationship.

- **Measurement Model:**

In the next step, the measurement model is derived using cause-effect relations identified in the previous modelling step. The measurement model now relates *indications* or *observations* made by the sensor to the measurand. In most cases, it is not necessary to develop the measurement model in full detail. Rather, a coarse overview of the processing steps involved in the measurement process is sufficient as the next step in the modelling procedure aims at a fully qualified uncertainty model.

- **Model Equation:**

The model equation relates all observations and other input quantities to the measurand. This core equation of the metrological system includes all quantities and their respective uncertainties. This step can be simplified by developing a graphical model. Due to the fact that all geometric quantities in our frame-work are represented by Gaussian random variables and linear transformations thereof are again Gaussian random variables, the graphical model<sup>5</sup> is composed of a small number of building blocks as outlined in Figure 10. We distinguish between the following blocks:

- *Source:* Uncertain quantity characterised by its best estimate and the uncertainty matrix. The source block is frequently used to represent prior information.
- *Transformation using constant parameters:* Simple transformations such as scaling functions are covered by this more general class of transformations. The uncertainty of the output quantity is only caused by the uncertainty of the input quantity.
- *Transformation of uncorrelated quantities:* Transformations with stochastic parameters extend the previous building block by the ability to model uncertainty contributions caused by uncertainties of the parameters. Examples for this class of transformations are geometric constructions such as the intersection of two lines resulting in an uncertain point. The lack of correlation between the input quantities is depicted by input quantities that enter the block on different sides or equivalently by small rectangles attached to the input quantities denoting the range of correlated quantities.
- *Transformation of correlated quantities:* As opposed to the previous class of transformations, this block explicitly covers correlations between quantities. Examples of this class of transformations are geometric constructions using entities which are based on a common source of uncertainty such as points commonly subjected to uncertain lens distortion. Graphically, correlation is indicated by grouping all correlated input quantities onto the same side of the block.

<sup>5</sup> We note that the terminology graphical model here refers to a simple and intuitive visualisation concept rather than to a model representation as used in the machine learning literature.



In summary, the components of the graphical model and their respective laws for the propagation of uncertainties are shown in Figure 10. Our set of components is chosen to allow for a straight forward derivation of the measurement equation. In contrast to Sommer & Siebert (2006), we explicitly differentiate between transformations using deterministic and stochastic parameters. We further consider parameter correlations in the graphical model and include the Bayesian information update into the modelling process.

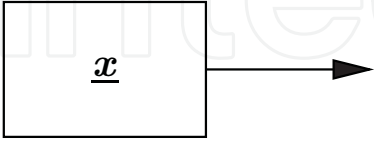
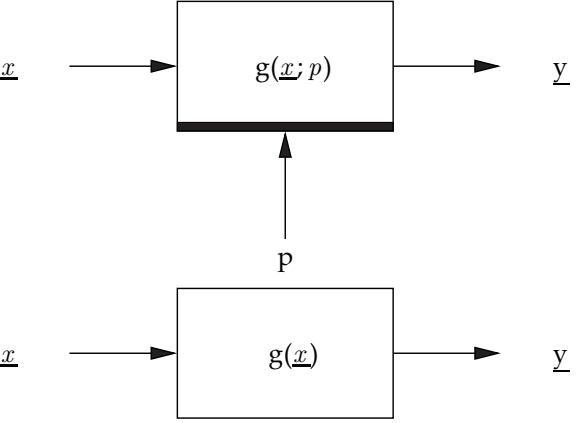
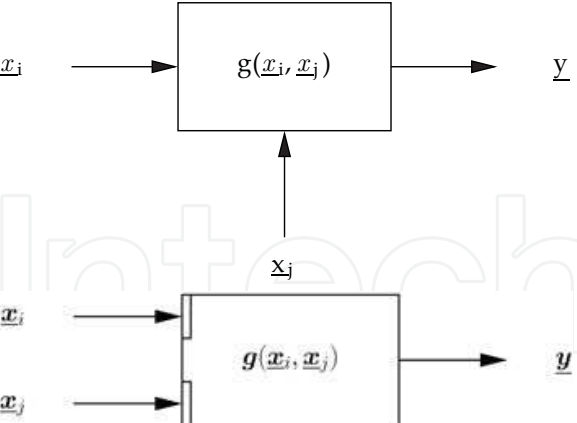
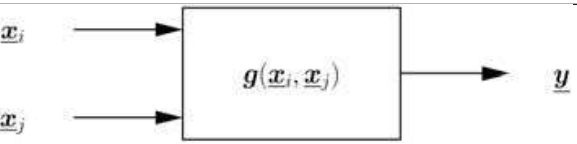
Symbol	Uncertainty Contribution
Source	
	$\Sigma_{xx}$
Transformation with constant parameters	
	$\Sigma_{yy} = J_g \Sigma_{xx} J_g^T$
Transformation of uncorrelated quantities	
	$\Sigma_{yy} = J_{g,x_i} \Sigma_{x_i x_i} J_{g,x_i}^T + J_{g,x_j} \Sigma_{x_j x_j} J_{g,x_j}^T$
Transformation of correlated quantities	
	$\Sigma_{yy} = J_g \begin{bmatrix} \Sigma_{x_i x_i} & \Sigma_{x_i x_j} \\ \Sigma_{x_j x_i} & \Sigma_{x_j x_j} \end{bmatrix} J_g^T$

Fig. 10. Building blocks of the graphical model. Uncertainty contributions are expressed by means of their respective uncertainty matrices. The matrices  $J$  denote the Jacobians of the respective transformation functions.

### 4.3 Limitations of the approach

The transformation of Gaussian quantities results in another Gaussian quantity only for linear transformations. As soon as the transformation exhibits a non-linear contribution, the resultant quantity starts to deviate from the Gaussian assumption with the degree of deviation depending on the degree of non-linearity introduced by the transformation function. From the metrological point of view, these deviations from the Gaussian are of concern for the following reasons:

1. Non-linearities cause the PDF of the output quantity to deviate from the Gaussian shape. This might effect reasoning modules which operate based on the Gaussian assumption.
2. The analytic derivations of Bayes' law are only applicable to Gaussian quantities. Any deviation from this Gaussian assumption will lead to approximate solutions and, therefore, inaccurate uncertainty estimates.
3. Non-linearities introduce a bias of the best estimate of the output quantity. The bias generally is a function of the best estimates of the input quantities as well as of the input uncertainties.

These effects usually strongly depend on the degree of correlation between the input quantities. A detailed discussion of situations where our approach fails due to one of the above listed causes is given in Brandner (2009).

## 5. Application example

In the present section we apply the presented modelling procedure to the estimation of homography parameters. The resultant processing block is further applied to a vision-based creep test sensor. We briefly outline the measurement model of this sensor in order to highlight some properties of the proposed modelling approach.

### 5.1 2D Homography with uncertainties

Among the family of perspective transformations, *2D homographies* relate coplanar points to their respective images under a central projection. In other words, a set of coplanar homogeneous points  $\mathbf{a}_i = (a_{x,i}, a_{y,i}, a_{h,i})^T$  in  $\Pi_1$  is mapped onto another set of coplanar points  $\mathbf{b}_i = (b_{x,i}, b_{y,i}, b_{h,i})^T$  in  $\Pi_2$  for  $i = 1, \dots, N$  as sketched in Figure 11a. Algebraically, corresponding tuples of points in  $\Pi_1$  and  $\Pi_2$  are related to each other by

$$\mathbf{b}_i = H\mathbf{a}_i \quad (21)$$

where the  $3 \times 3$  matrix  $H$  is a 2D homography and defined up to a scalar factor. Thus,  $H$  has 8 degrees of freedom (cf. Hartley & Zisserman (2004), p. 44). Consequently, the equality in Equation 21 is defined up to a non-zero scaling factor. In a metrological context, homographies can be used to model geometric constellations where features are bound to positions within a know plane (Ma et al. (2005); Stuflessner & Brandner (2008); Brandner et al. (2008)). Stacking the elements of the homography matrix  $H$  into a column vector  $\mathbf{h}$  allows us to rewrite Equation 21 to obtain

$$G\mathbf{h} = 0, \quad (22)$$

where the matrix  $G$  depends on the input points in both planes. In the case of  $N = 4$  point pairs in non-degenerate configurations (cf. Hartley & Zisserman (2004)) the non-trivial

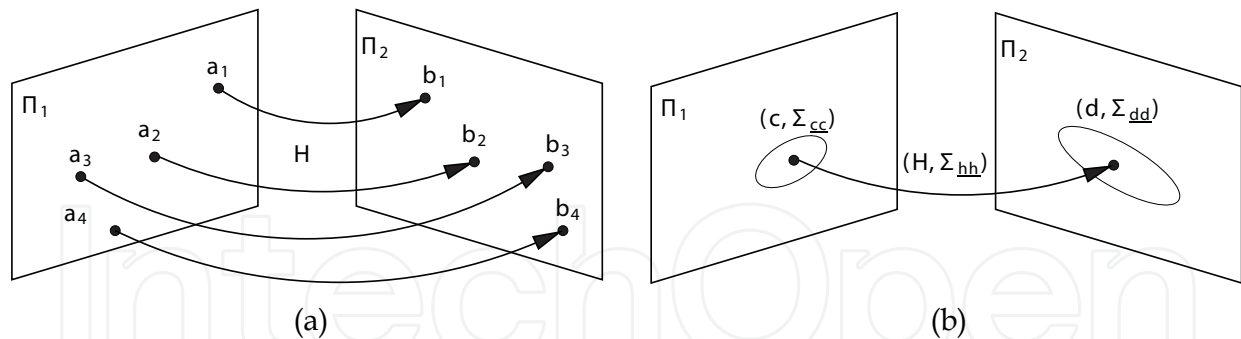


Fig. 11. Planar homography as a special case of a perspective transformation. (a) The homography  $H$  relates coplanar points  $\mathbf{a}_i$  in  $\Pi_1$  to their coplanar image points  $\mathbf{b}_i$  in  $\Pi_2$ . (b) Given an uncertain point  $(\mathbf{c}, \Sigma_{cc})$  and the parameters of the homography including their uncertainties  $(H, \Sigma_{hh})$ , the resultant point and its associated uncertainty  $(\mathbf{d}, \Sigma_{dd})$  can be obtained using first order uncertainty propagation (see text).

solution to the system in Equation 22 is exact. For the case of  $N > 4$  the system is over-determined. Taking into account uncertainties of the input quantities, the solution in general is only approximate. Different optimisation strategies are known to numerically solve Equation 22. A representative of linear, direct least-squares estimators is the *Direct Linear Transform* (DLT) estimator. The cost functional minimised by the DLT is an *algebraic distance*. Due to its simplicity and numerical stability the DLT algorithm is widely used for homography estimation. The algorithm solves the system  $G\mathbf{h} = 0$  for non-trivial solutions, i.e. solutions  $\mathbf{h} \neq 0$ , by minimising  $\|G\mathbf{h}\|$ . In order to avoid trivial solutions the minimization procedure is subjected to the constraint  $\|\mathbf{h}\| = c$  for an arbitrary non-zero constant  $c$ . Although the exact value of  $c$  is irrelevant to the estimation process it is commonly set to  $c = 1$  which can be realised by a norm constraint within the optimisation target, i.e.

$$\frac{\|G\mathbf{h}\|}{\|\mathbf{h}\|} \rightarrow \min. \quad (23)$$

The solution of the minimisation problem in Equation 23 is given by the eigenvector that corresponds to the smallest eigenvalue of  $M = G^T G$  (cf. Hartley & Zisserman (2004)). A numerically robust solution is obtained via singular value decomposition (SVD) of  $M$ . We now cover uncertain input quantities as well as homography parameter uncertainties. Consider the example shown in Figure 11b: An input data point  $\mathbf{c}$  is transformed from plane  $\Pi_1$  onto plane  $\Pi_2$  using the homography  $H$ . The different sources of uncertainty contributing to final point estimate  $\mathbf{d}$  are summarised in the cause-effect diagram shown in Figure 12. Using the processing blocks introduced in the previous section we can sketch the measurement model as shown in Figure 13a. This special configuration is characterised by the complete absence of any inter-parameter correlation. The resultant uncertainty of the output quantity  $\mathbf{d}$  can be derived using

$$\Sigma_{dd} = H \Sigma_{cc} H^T + B_c \Sigma_{hh} B_c^T, \quad (24)$$

where  $B_c$  represents an appropriate Jacobian function. Equation 24 greatly simplifies analytical derivations and, therefore, is frequently used by researchers in the field to

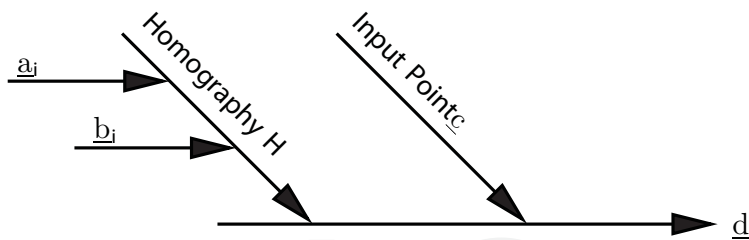


Fig. 12. Cause-effect diagram of the point measurement application shown in Figure 11b. Both uncertainties of the points used to estimate the homography parameters and uncertainties of the input point  $\underline{c}$  contribute to the uncertainty of  $\underline{d}$ .

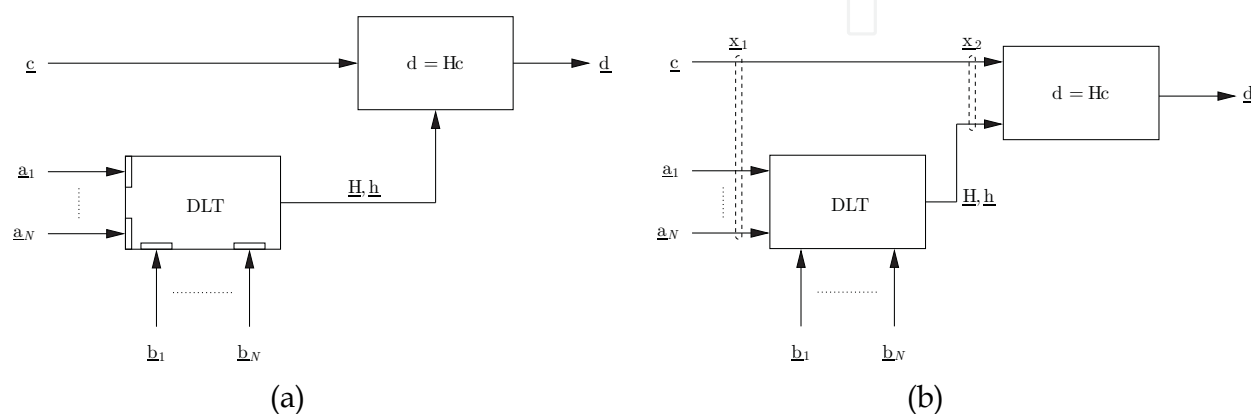


Fig. 13. Graphical models of a measurement application based on a 2D/2D homography as shown in Figure 11b for different degrees of correlations between the involved parameters. Two point sets  $\underline{a} = \{\underline{a}_i\}$  and  $\underline{b} = \{\underline{b}_i\}$  are used to estimate  $H$ . This homography is in turn used to map a point  $\underline{c}$  onto its image  $\underline{d}$ . (a) All contributing parameters are uncorrelated. (b) Common situation in planar metrology: The point set  $\underline{a}$  and  $\underline{c}$  are acquired simultaneously resulting in parameter correlation.

propagate uncertainties (cf. Criminisi (2001)). Apart from neglecting correlations between transformation parameters and geometric entities that are being mapped, Criminisi (2001) also assumes statistical independence within the point sets  $\underline{a}_i$  and  $\underline{b}_i$  that are used to estimate the homography parameters.

Correlations between parameters are often caused by uncertainties common to two or more quantities or by un-modelled systematic effects. A frequent source of systematic effects in computer vision are geometry-based biases in feature detectors. Thus, a more appropriate model for the homography example is given in Figure 13b. Apart from allowing for intra-parameter correlations within the set of model points  $\underline{a}_i$ , the model also covers correlations between the model points and the test point  $\underline{c}$ . This situation occurs during *single acquisition* measurements, i.e. both the points used to estimate the homography parameters and the points used to apply the homography are detected within the same image. Under such circumstances, correlations need to be considered. It can be shown (cf. Brandner (2009)) that the measurement uncertainty of the resultant point  $\underline{c}$  is obtained by

$$\Sigma_{\underline{d}\underline{d}} = J \begin{bmatrix} \Sigma_{\underline{c}\underline{c}} & \Sigma_{\underline{c}\underline{a}} K_a^T \\ K_a \Sigma_{\underline{c}\underline{a}}^T & \Sigma_{\underline{h}\underline{h}} \end{bmatrix} J^T, \tag{25}$$

where  $J$  represents a Jacobian matrix and  $K_a$  a weighing matrix, respectively. By inspection of Equation 25 we observe that the correlations between the point sets  $\mathbf{a}_i$  and  $\mathbf{c}$  enter the uncertainty calculi via their respective covariance matrix. The correlation introduced by the application of the homography is taken into account by means of the transformation  $J$ .

### 5.1.1 A numerical example

In order to validate the implementation of the previously described method to analytically estimate both the homography parameters and their associated uncertainties we compare the results with the estimates obtained using a Monte Carlo analysis. Figure 14 depicts a sample image where corner features are used to estimate the homography between the planar target and the image plane. The corners are detected and their respective positions  $\mathbf{b}_i$  are estimated using a morphological detector. In this experiment an isotropic additive Gaussian noise source with variance  $\sigma^2 = 1\text{pixel}^2$  is superimposed to the true corner positions. Thus, assuming equal noise properties for each corner the covariance of  $\mathbf{b}_i$  is given by

$$\Sigma_{\mathbf{b}_i\mathbf{b}_i} = \Sigma_{\mathbf{b}\mathbf{b}} = \begin{bmatrix} 1 & 0 \\ 0 & 1 \end{bmatrix}. \quad (26)$$

Similarly we assume that the model uncertainty is characterised by an isotropic additive Gaussian noise source with variance  $\sigma^2 = 0.01\text{cm}^2$ . The four corners of the rectangle and the lower-left corner of the triangle are used to estimate the homography  $H$  and the associated covariance matrix  $\Sigma_{\mathbf{h}\mathbf{h}}$ . The red ellipses in Figure 14a represent the 95% probability regions around each detected corner. Clearly, the point correspondences used to estimate the homography show smaller deviations compared to other points which did not contribute to the estimation result. The close-up in Figure 14b shows a comparison of the analytic result with empirical moments obtained via MC simulation. The red ellipse again represents the 95% probability region based on the analytic estimate of the homography covariance whereas the dashed blue line represent the same probability region based on  $N = 10^4$  MC iterations. Both uncertainty estimates are in good agreement justifying the application of the analytic approach.

### 5.2 2D displacement measurement

Using the results of the previous discussion, we can now derive the uncertainty model of a 2D displacement measurement system which reflects the general structure of a vision-based metrological system as shown in Figure 4. The measurement system is part of a creep test apparatus used to obtain material parameters of polymer samples under specific conditions. The experimental setup and the measurement system are explained in more detail in Brandner et al. (2008). Figure 5a shows the practical realisation of this sensor. Care has been taken to consider environmental conditions that include the submersion of the material samples in tempered oil. Our focus in this section is to justify the particular uncertainty model applied for this measurement system.

Figure 15 depicts the geometric sketch of the displacement measurement system. A single camera is used to acquire an image of a scene comprising a planar reference target and a planar sample target. These targets each consists of circular blob features manufactured into

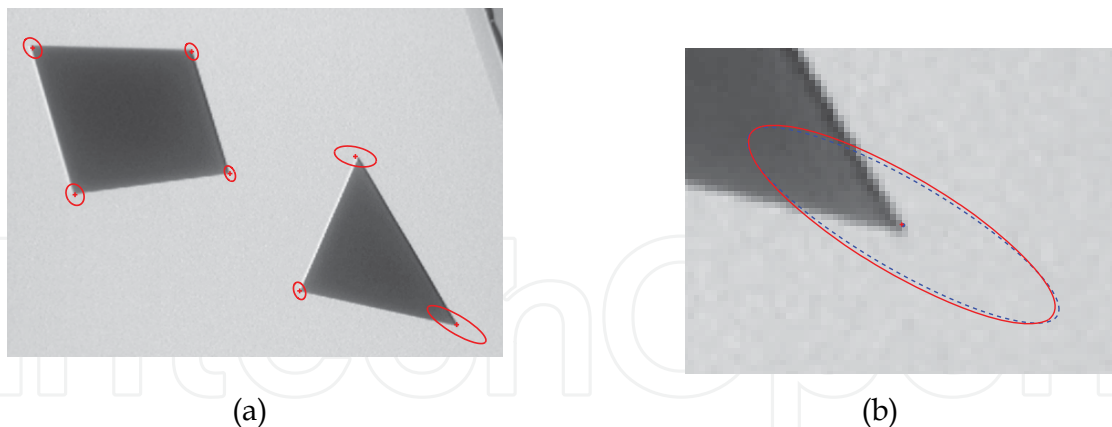


Fig. 14. Direct linear estimation of the homography parameters that relate the seven corners with corresponding point positions in a model database. (a) The four corners of the rectangle and the lower-left corner of the triangle are used to estimate the homography parameters. The ellipses depict the 95% probability regions of the predicted image corners based on model-, feature detection-, and homography parameter uncertainty. (b) Comparison of the analytic method with a Monte Carlo simulation. The close-up of the lower-right corner of the triangle shows that due to the close agreement the Monte Carlo results support our analytical estimates.

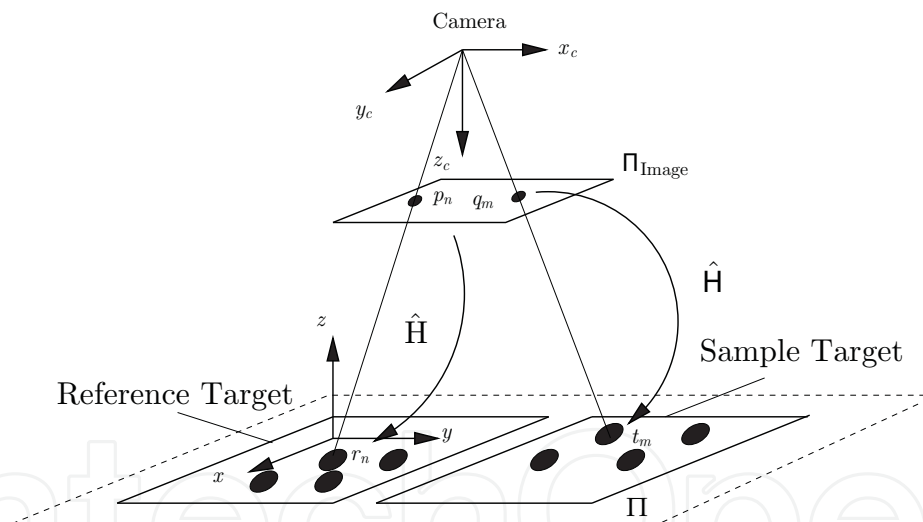


Fig. 15. Outline of the geometry of a single camera/target pair. This *single image acquisition* setup processes the same image twice: First, features on the reference target are used to estimate the transformation parameters  $\hat{H}$ . Second, these parameters are applied to features on the sample target in order to estimate the displacement of this target.

a stainless steel sheet by laser marking. By construction of the setup, the two targets are coplanar so that a homography  $\hat{H}$  can be used to relate the image plane of the sensor  $\Pi_{\text{Image}}$  to the ( $z = 0$ )-plane which holds both targets. During the measurement process a single image is used to simultaneously obtain image points corresponding to the reference target and the sample target. Based on these image points, the sensor estimates the parameters of the homography which are then used to reconstruct the 2D displacement of the sample target with respect to the reference target.

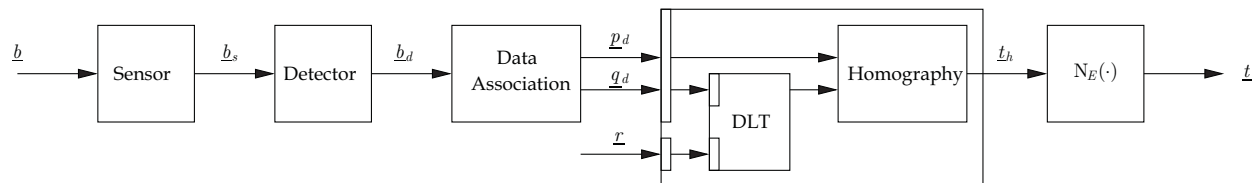


Fig. 16. Uncertainty model of the 2D displacement measurement system. The simultaneous estimation and application of the homography parameters require the proper handling of correlations.

For this specific measurement application we note that each image point is mapped by the same sensor and detected under the same illumination conditions of the scene. The common sensor calibration as well as common systematic effects such as ageing of the medium introduce a correlation between the points used to estimate the homography and the points which are transformed using the estimated homography.

Figure 16 shows the graphical model relating the input quantities (i.e. the image centres of the blobs) to the measurand (i.e. the position  $t$  in metric coordinates). This model graphically represents the measurement equation. Note that we explicitly visualise parameter correlations which is shown by the following two examples: First, the estimation of the homography parameters is performed using the direct linear transform algorithm (DLT, Hartley & Zisserman (2004)). This algorithm takes as input a sequence of image points,  $q_d$  and their corresponding model points  $r$ . While the image points are correlated due to their common acquisition conditions, no dependency between the image points and their models is considered in this model. This is denoted by the two rectangles within the DLT block restricting correlations to appear *within* the rectangle only. Second, the final homography parameters are used to map the image point  $p_d$  in order to obtain  $t_h$ . The common acquisition of  $p_d$  and  $q_d$  gives rise to a inter-parameter correlation between the input parameters to the homography block. The rectangle corresponding to the range of correlated input quantities is now extended to all quantities entering the block on the right – and, consequently, omitted for a clear representation. We can straight forwardly nest different layers of the model in order to better visualize relevant effects. This is shown with an aggregate model block enclosing both the DLT estimator and the homography application indicating the relevant parameter correlations at its inputs.

## 6. Summary

This paper addresses the problem of measurement uncertainty evaluation in vision-based measurement applications. We contribute to the state of the art by the development of a consistent frame-work for the modelling of uncertainties in vision-based applications. By combining the Gaussian representation of geometric entities in perspective spaces with the current Bayesian extensions of the Guide to the Expression of Uncertainty in Metrology (GUM) we introduce the concept of a *metrological geometry*. We identify a set of simple graphical building blocks which serve to characterise and to quantify the measurement uncertainty of the metrological application in a step-by-step approach. The presented frame-work is applicable to Gaussian quantities and transformation functions that are linear or that can be locally linearised. Using homogeneous coordinates, many constructions of entities are based on bilinear transforms which are well suited for local linearisation.

All input quantities contributing to the measurement uncertainty of the final result can be covered by the proposed frame-work. These include the calibration parameters of the sensor as well as the uncertainty introduced by transformations.

The presented work enables improvements for applications involving the analysis of measurement uncertainties in different ways: First, the presented building blocks provide an easy-to-use and intuitive way to visualise all quantities involved in the measurement process. They further explicitly highlight parameter correlations which are important to take into consideration when evaluating measurement uncertainties.

Second, the analytical derivation of the measurement uncertainty for most applications is computationally far less intensive than comparable alternatives such as Monte Carlo simulations. This allows for the construction of algorithms which determine the uncertainty of any measurement result in real-time *including* the incorporation of the best estimate. The resultant uncertainty estimates provide tighter interval boundaries which increases the usefulness of the result.

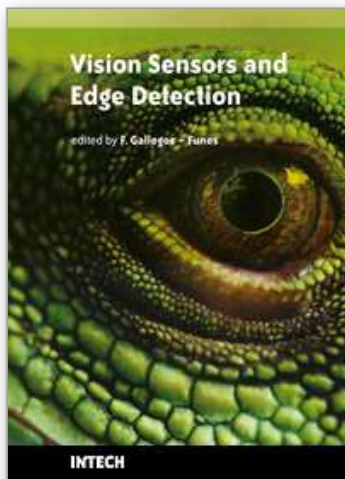
Third, correlations between quantities contributing to the measurement result are fully covered by the frame-work. As shown in the application section, the parameters of homographies can straight forwardly be estimated based on and applied to correlated features. Thus, mis-estimates of the measurement uncertainty based on false independence assumptions can be avoided. This paper extends prior work by Criminisi (2001) which targets the derivation of parameter uncertainties of 2D/2D homographies. We cover correlations within the input entities of the DLT estimator as well as correlations between the homography parameters and their respective input parameters. This allows us to tackle single image acquisition scenarios as frequently encountered in vision-based metrology.

## 7. References

- BIPM (2006). *The International System of Units (SI)*, 8 edn, Bureau International des Poids et Mesures (BIPM).
- BIPM (2008). Convention du Mètre. [http://www.bipm.org/en/convention\(07/2008\)](http://www.bipm.org/en/convention(07/2008)).
- Brandner, M. (2006). Uncertainty estimation in a vision-based tracking system, *Proceedings of the IEEE Intl. Workshop on Advanced Methods for Uncertainty Estimation in Measurement (AMUEM 2006)*, Sardinia, Italy, pp. 40–45.
- Brandner, M. (2009). *Uncertainty Evaluation in Vision-Based Measurement Systems*, PhD thesis, Graz University of Technology.
- Brandner, M., Thurner, T., Kukutschki, G. & Enzinger, N. (2008). Optical 2D displacement and strain sensor for creep testing of material samples in transparent fluids, *Instrumentation and Measurement Technology Conference Proceedings - IMTC2008*, Victoria, Vancouver Island, Canada, pp. 1419–1423.
- Criminisi, A. (2001). *Accurate Visual Metrology from Single and Multiple Uncalibrated Images*, Springer.
- DIN1319 (1995). *Fundamentals of Metrology - Part 1: Basic Terminology*, Deutsches Institut für Normung (DIN). DIN1319-1: 1995-01.
- Frstner, W. (2004). Statistics in projective geometry, Tutorial given at the European Conference on Computer Vision (ECCV).
- Gelman, A., Carlin, J. B., Stern, H. S. & Rubin, D. B. (2003). *Bayesian Data Analysis*, Chapman and Hall/CRC. ISBN 1-58466-388-X.



- Hartley, R. I. & Zisserman, A. (2004). *Multiple View Geometry in Computer Vision*, 2<sup>nd</sup> edn, Cambridge University Press.
- Havelock, D. I. (1989). Geometric precision in noise-free digital images, *IEEE Transactions on Pattern Analysis and Machine Intelligence* 11(10): 1065–1075.
- Heuel, S. (2003). *Uncertain Projective Geometry: Statistical Reasoning for Polyhedral Object Reconstruction*, number 3008 in *Lecture Notes in Computer Science*, Springer.
- VIM (1993). *International vocabulary of basic and general terms in metrology*, International Organization for Standardization (ISO), Geneva, Switzerland.
- Iuculano, G., Zanobini, A., Lazzari, A. & Gualtieri, G. P. (2003). Measurement uncertainty in a multivariate model: A novel approach, *IEEE Transactions on Instrumentation and Measurement* 52(5): 1573–1580.
- Iversen, G. R. (1984). *Bayesian Statistical Inference*, number 07-043 in *Quantitative Applications in the Social Sciences*, Sage University Paper.
- Jaynes, E. T. (1968). Prior probabilities, *IEEE Transactions on Systems Science and Cybernetics* 4(3): 227–241.
- JCGM (2008a). Evaluation of measurement data - Guide to the expression of uncertainty in measurement, *Technical Report JCGM 100:2008*, Joint Committee for Guides in Metrology.
- JCGM (2008b). Evaluation of measurement data - Supplement 1 to the Guide to the expression of uncertainty in measurement - Propagation of distributions using a Monte Carlo method, *Technical Report JCGM 101:2008*, Joint Committee for Guides in Metrology.
- Kacker, R. & Jones, A. (2003). On use of Bayesian statistics to make the Guide to the Expression of Uncertainty in Measurement consistent, *Metrologia* 40: 235–248.
- Kanungo, T., Jaisimha, M., Palmer, J. & Haralick, R. (1995). A methodology for quantitative performance evaluation of detection algorithms, *IEEE Transactions on Image Processing* 4(12): 1667–1674.
- Lira, I. (2001). *Evaluating the Measurement Uncertainty*, Series in Measurement Science and Technology, Institute of Physics Publishing, Bristol and Philadelphia.
- Ma, Y., Soatto, S., Kosecka, J. & Sastry, S. S. (2005). *An Invitation to 3-D Vision*, Springer. ISBN 0387008934.
- Ochoa, B. & Belongie, S. (2006). Covariance propagation for guided matching, *Statistical Methods in Multi-Image and Video Processing*, Graz, Austria.
- Papoulis, A. & Pillai, S. U. (2002). *Probability, random variables, and stochastic processes*, 4<sup>th</sup> edn, McGraw-Hill.
- Sommer, K. D. & Siebert, B. R. L. (2006). Systematic approach to the modelling of measurements for uncertainty evaluation, *Metrologia* 43: 200–210.
- Stuflesser, M. & Brandner, M. (2008). Vision-based control of an inverted pendulum using cascaded particle filter, *IEEE Instrumentation and Measurement Technology Conference*, Victoria, Canada, pp. 2097–2102.
- Triggs, B. (2001). Joint feature distributions for image correspondence, *Proceedings of the International Conference on Computer Vision*, pp. 101–108.
- Weise, K. & Wöger, W. (1999). *Meßunsicherheit und Meßdatenauswertung*, Wiley-VCH. ISBN 3-527-29610-7.



## **Vision Sensors and Edge Detection**

Edited by Francisco Gallegos-Funes

ISBN 978-953-307-098-8

Hard cover, 196 pages

**Publisher** Sciyo

**Published online** 12, August, 2010

**Published in print edition** August, 2010

Vision Sensors and Edge Detection book reflects a selection of recent developments within the area of vision sensors and edge detection. There are two sections in this book. The first section presents vision sensors with applications to panoramic vision sensors, wireless vision sensors, and automated vision sensor inspection, and the second one shows image processing techniques, such as, image measurements, image transformations, filtering, and parallel computing.

### **How to reference**

In order to correctly reference this scholarly work, feel free to copy and paste the following:

Markus Brandner (2010). Bayesian Uncertainty Evaluation in Vision-Based Metrology, Vision Sensors and Edge Detection, Francisco Gallegos-Funes (Ed.), ISBN: 978-953-307-098-8, InTech, Available from: <http://www.intechopen.com/books/vision-sensors-and-edge-detection/bayesian-uncertainty-evaluation-in-vision-based-metrology>

**INTECH**  
open science | open minds

### **InTech Europe**

University Campus STeP Ri  
Slavka Krautzeka 83/A  
51000 Rijeka, Croatia  
Phone: +385 (51) 770 447  
Fax: +385 (51) 686 166  
[www.intechopen.com](http://www.intechopen.com)

### **InTech China**

Unit 405, Office Block, Hotel Equatorial Shanghai  
No.65, Yan An Road (West), Shanghai, 200040, China  
中国上海市延安西路65号上海国际贵都大饭店办公楼405单元  
Phone: +86-21-62489820  
Fax: +86-21-62489821

© 2010 The Author(s). Licensee IntechOpen. This chapter is distributed under the terms of the [Creative Commons Attribution-NonCommercial-ShareAlike-3.0 License](https://creativecommons.org/licenses/by-nc-sa/3.0/), which permits use, distribution and reproduction for non-commercial purposes, provided the original is properly cited and derivative works building on this content are distributed under the same license.

IntechOpen

IntechOpen